Application Notes

Mohamed Abdel-Mottaleb and
Mohammad H. Mahoor
University of Miami, USA

Algorithms for Assessing the Quality of Facial Images

I. Introduction

Video surveillance cameras are installed in public places of many cities such as Jersey City, New Orleans, Chicago, and Los Angles in the US and in many locations around the world. The City of Tampa, Florida, used face recognition technology during the 2001 Super Bowl. The State of Colorado is scanning the photos of drivers' licenses into a database to match against criminal mug shots on file nationwide. "Despite complaints by privacy advocates, the number of surveillance cameras is growing and proving increasingly valuable to police for catching criminals as well as protecting against terrorists" [13]. With the tremendous increase in the number of installed video surveillance cameras and the deployment of face-recognition software, the demand for high performance face recognition systems is obvious.

In 2005, US-VISIT's [3] study showed that most of the poor quality fingerprints encountered from frequent US-VISIT travelers were not from individuals with intrinsically poor fingerprints (nicknamed "goats"), but were instead due to collection problems. The quality of captured biometric data can be improved by better sensors, better user interfaces, or by compliance with standards [5]. In the past few years, researchers developed algorithms to measure the quality of fingerprint images [12], [7] and iris images [8].

The National Institute of Standards and Technology (NIST) addressed this problem in August 2004 when it published the NIST Fingerprint Image Quality algorithm, which was designed to be predictive of the performance of minutiae matchers [17]. Since then, NIST has been considering how quality measures should be evaluated, developing quality measures for other biometrics, and considering the wider use of such measures. Recently, NIST had a workshop to present the state of the art in this field [1]. The importance of facial image quality and its effects on the performance of face recognition systems was also considered by Face Recognition Vendor Test (FRVT) protocols [14], [2]. In face recognition systems, many factors such as blurring effect, facial expressions, lighting conditions, head pose, and facial hair could affect the quality of the facial images. These factors could affect both the Holistic and the Geometric based face recognition techniques.

In this paper, we develop algorithms for assessing the quality of facial images with respect to the effects of *blurring, lighting conditions, head pose, and facial expressions*. These algorithms can be used in the *Quality Assessment* (Q.A.) module of a face recognition system (Figure 1). As shown in Figure 1, one role of Q.A. is to assess the quality of facial images to either reject or accept them for the recognition step. Quality assessment can also be used to assign weights to different face recognition algorithms in a fusion scheme. In order to develop algorithms for assessing the quality of facial images, the challenge is to measure the level or the intensity of the factors that affect the quality of the facial images. For example, a facial image could have an expression intensity ranging from neutral to maximum. Obviously, the recognition of a facial image with exaggerated expressions is more difficult than the recognition of a facial image with a light expression. For blurring, lighting conditions, and head pose effects, measuring the level of these factors is possible. But, measuring the intensity of a face expression is difficult because of the absence of a reference neutral face image.

Considering the issues discussed above, we take two different strategies to assess the quality of facial images: one strategy for blurring, lighting conditions, and head pose effects and another strategy for facial expressions. In the first strategy, we define measures that correlates with the level of degradation of the captured facial images. Based on each measure, we define a polynomial function for predicting the performance of the Eigenface [18] technique on a given image; and then by selecting a suitable threshold for the predicted recognition rate, we accept or reject the image for recognition. In the second strategy for

1556-603X/07/$25.00©2007IEEE

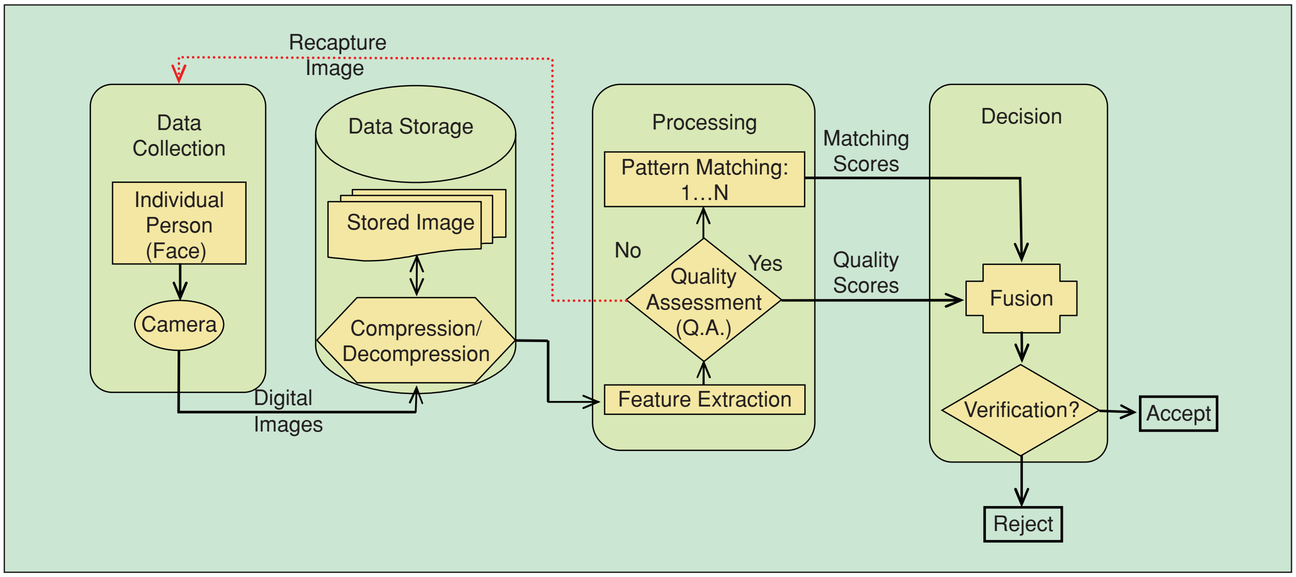

FIGURE 1 General block diagram of a biometric system.

facial expressions, where measuring the intensity of an expression is difficult, we classify a given image into one of two classes, i.e., "Good quality," or "Poor quality." The training for these classes is achieved by dividing a training set of facial images into two subsets based on whether the images are recognizable by the Eigenface technique or not. Then these two subsets are described by Gaussian Mixture Models (GMMs).

The rest of this paper is organized as follows: Section II introduces the algorithms for assessing the quality of facial images affected by blurring, lighting conditions, head pose, and facial expressions. Section III presents the experimental results. Conclusions and the future works are discussed in Section IV.

II. Algorithms for Assessing the Quality of Facial Images

In this Section, we present our algorithms for assessing the quality of facial images, with respect to blurring, lighting conditions, head pose, and facial expressions. We assume that an image is only affected by one factor.

A. Blurring Effect Assessment

To assess the quality of facial images with respect to blurring, we develop a measure that correlates with the intensity of blurriness. Based on this measure, we define a function to predict the recognition rate of the Eigenface technique. One approach for measuring the blurring or sharpness of an image is to analyze the image in the frequency domain. An image with sharp edges and without blurring effects has more energy at the higher spatial frequencies of its Fourier transform than a blurred version of that image. In other words, an image with fine details and edges has flatter 2-D spatial frequency response than a blurred image. The blurring effect attenuates the high spatial frequency contents of an image. In order to assess the energy of the high frequency content of an image, one approach is to analyze the image in the Fourier domain using statistical analysis. One statistical measure that can be used for this purpose is Kurtosis. In the following subsection, we review the Kurtosis measure. Then, in the last subsection, we obtain a function that predicts the performance rate of Eigenface technique on a given image based on the blurriness of the image.

1) Measuring Image Sharpness Using the Kurtosis Measure: An elegant approach for measuring electron microscope image sharpness is presented in [19]. This approach computes a measure based on the statistical analysis of the Fourier transformation of the image. Kurtosis is a measure of the departure of a probability distribution from Gaussian (normal) distribution with unit variance. For a one dimensional random variable x with mean μ_x, the Kurtosis is defined as [10]:

$$\kappa = m_4/m_2^2 \qquad (1)$$

where m_4 and m_2 are the fourth and the second moments, respectively, defined as: $m_4 = E[(x-\mu_x)^4]$ and $m_2 = \sigma_x^2 = E[(x-\mu_x)^2]$. For a normal distribution with unit variance, the value of κ is 3. If the value of κ, for a given distribution, is less (or greater) than 3, then the distribution is "flat-topped" (or "peaked") relative to a Gaussian. In other words, the smaller the value of the Kurtosis, the flatter the distribution. For a multi-dimensional random variable, Y, the Kurtosis is defined as:

$$\kappa = E[(Y-\mu_Y)^t \Sigma^{-1} (Y-\mu_Y)]^2 \qquad (2)$$

where Σ is the covariance matrix and μ_Y is the mean vector.

In this work, we use the value of Kurtosis (Eq. 2) for predicting the face recognition rate. Our experiments show that the Kurtosis measure has a linear response within a wide range of blurring effects (Figure 2). In the experiments for blurring effect assessment, the facial images

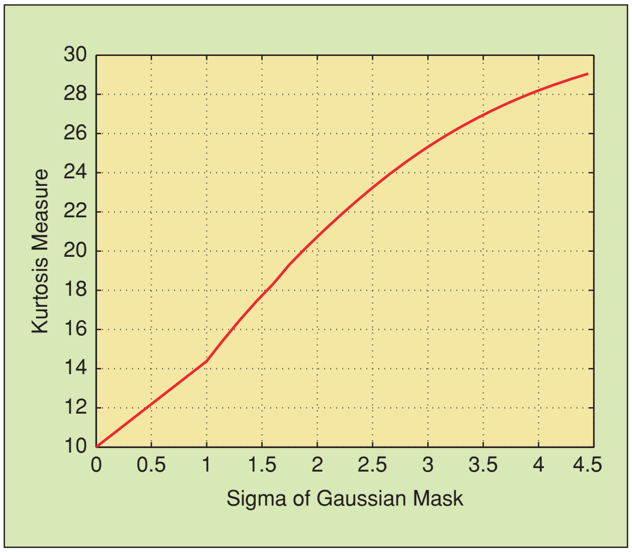

FIGURE 2 Kurtosis measure versus different value of σ for Gaussian mask.

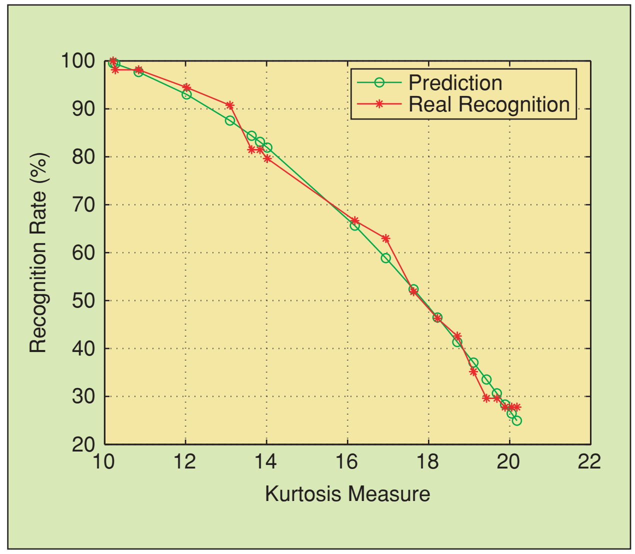

FIGURE 3 Recognition rate of the Eigenface technique versus Kurtosis measure.

were blurred using a Gaussian mask with different values of the standard deviation σ. The average value of the Kurtosis for facial images without blurring is 10 and it increases with larger values of σ.

2). Face Recognition Performance Prediction: Figure 3 shows the recognition rate of the Eigenface technique versus the Kurtosis measure. The Figure shows that the recognition rate decreases with larger values of the Kurtosis measure (i.e. higher blurriness). To assess the quality of a face image degraded by blurring, we define a polynomial function that predicts the recognition rate of the Eigenface from the Kurtosis measure. This function is obtained by applying regression to the data in Figure 3. By choosing a suitable threshold for the predicted recognition rate we can either accept or reject a given facial image for recognition. This procedure can be used to develop prediction functions for other face recognition techniques.

B. Lighting Effect Assessment

To assess the quality of facial images with respect to lighting conditions, we define a measure that represents the effect of scene illumination on captured facial images. Based on this measure, which we call *wmi*, a function is introduced to predict the recognition rate for a face image using the Eigenface technique. The *wmi* is obtained by calculating the weighted sum of the mean intensity values of the pixels in different regions of the face image. To calculate *wmi* for a given facial image, at first we normalize the intensity values of the image to zero mean and unit variance. Then we partition the image into 16 regions and calculate the mean intensity value of each region. Finally, we obtain the *wmi*, by calculating the weighted sum of the mean intensity values of the 16 regions in the image:

$$wmi = \sum_{i=1}^{16} w_i . \bar{I}_i \tag{3}$$

$$\bar{I}_i = \frac{1}{MN} \sum_{x=1}^{N} \sum_{y=1}^{M} I(x, y) \tag{4}$$

where, w_i is the weight factor for the *ith* region and $I(x, y)$ is the intensity value of the pixel at position (x, y) in the image. We use a Gaussian mask to weight different regions on the face. This has the effect of assigning large weights to the regions in the middle of the image and small weights to the regions in the borders of the image.

To assess the quality of a given facial image, we define a function that predicts the recognition rate of the Eigenface versus *wmi* measure. Figure 4 shows the recognition prediction function for the Eigenface technique. The coefficients of the prediction function were estimated by regression. It shows that for larger values of *wmi*, which correspond to a frontal light source, the Eigenface has a higher recognition rate.

We follow the same approach that we proposed for assessing the blurring effect. By choosing a threshold, we reject images that have predicted recognition rate lower than the threshold and accept images that have predicted recognition rate above the threshold.

C. Head Pose Effect Assessment

To assess the quality of facial images with respect to head pose orientation, we need to define a measure that correlates with the head pose. We assume that a suitable image for the face recognition technique under evaluation is a frontal facial image and the performance of the technique degrades with large changes in head pose orientation. We developed a measure that changes with the head *yaw* orientation. To calculate this measure, we locate three facial feature points: the centers of the eyes and the center of the mouth, using the algorithm in [6]. Then, the two areas of the facial skin S_L and S_R, which are shown in Figure 5, on the sides of the triangle formed by the three feature points are used to define the pose measure:

$$pm = \frac{S_L - S_R}{min(S_L, S_R)} \tag{5}$$

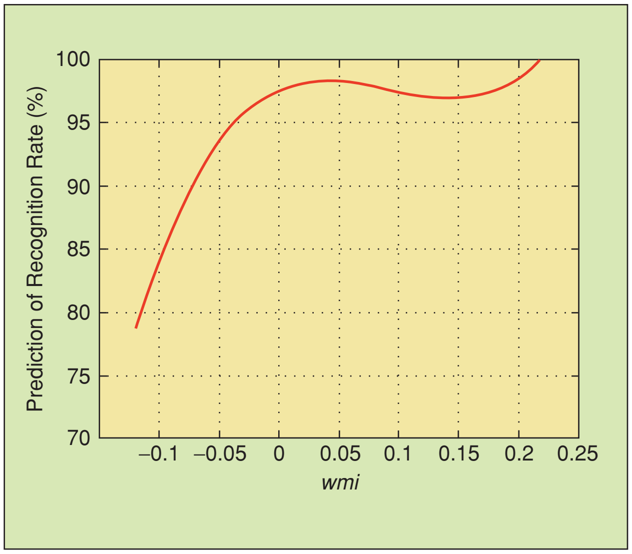

FIGURE 4 Prediction function for lighting conditions assessment: prediction recognition rate versus *wmi* measure.

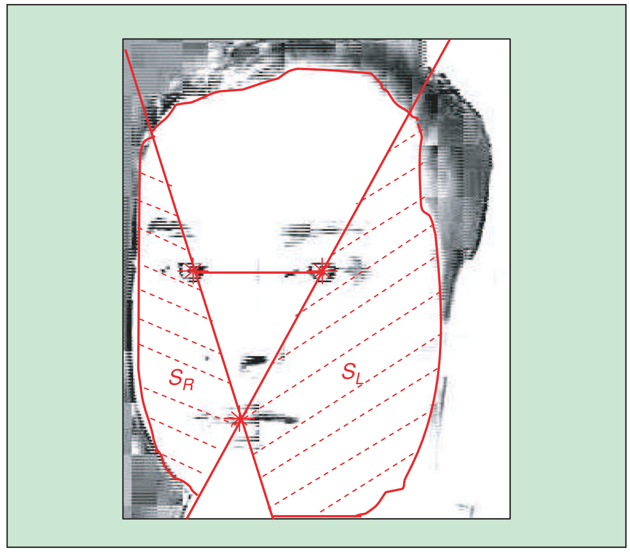

FIGURE 5 Head pose estimation using the skin area on the two sides of the triangle.

To discriminate between the skin color and other regions in the facial images such as hair and background, we use the Fisher Discriminant Analysis (FDA) technique. By applying FDA to each pixel of the color image, we can discriminate between the skin color and other regions such as hair. Because the lighting condition for the captured images under the test (i.e., the 2nd album of West Virginia University face database) is uniform from any point of view, therefore there is not noticeable shadow effect in these images and hence our technique for skin detection is robust. In case of shadow effect, the techniques that are based on normalized color spaces can be used to reduce the shadow effect during the skin detection process. We use the second album of face database of West Virginia University (WVU) [11] to test our algorithm. This album contains color face images of 50 subjects with head orientation, i.e., yaw angle, from −45 degrees to +45 degrees. Figure 6 shows the mean value of the pm measure versus the yaw angle for 50 subjects in our database. As the Figure shows, the pm measure is strongly correlated with the head orientation. To assess the quality of a face image degraded by head pose, we use the value of pm (Eq. 5) to predict the recognition rate of the Eigenface technique. The prediction function is obtained by regression of the data in Figure 7. By choosing a threshold, we reject images that have predicted recognition rate lower than the threshold and accept images that have predicted recognition rate above the threshold.

D. Facial Expressions Effect Assessment

For facial expression analysis, the temporal dynamics and intensity of facial expressions can be measured by determining either the geometric deformations or the density of wrinkles that appear in certain regions of the face [4]. Since there are interpersonal variations with regard to the amplitudes of the facial actions, it is difficult to determine the absolute intensity of the facial expression for a given subject without referring to an image of the neutral face of the subject. In this work, we assume that during the operation of the system we do not have the image of the neutral face of the subject, as a result, we follow a different approach from the one we use in blurring effect. Figure 8 shows a block diagram of our algorithm. In order to train the system, we use a database of facial images that contains for each subject an image with neutral face and images with different expressions with varying intensities. During training, we use the Eigenface recognition technique, for recognizing these facial images. The result of this step is two subsets of facial images: one subset contains images that could be recognized correctly, called "Good quality images," and the other subset contains images that could not be recognized correctly, called "Poor quality images."

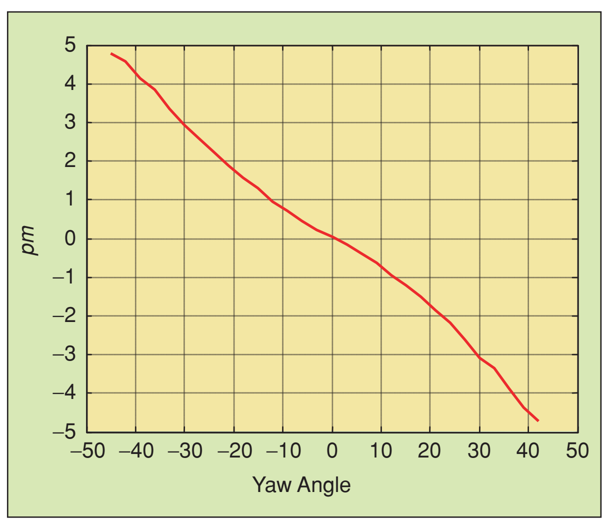

FIGURE 6 Head pose estimation using the skin area on the two sides of the triangle.

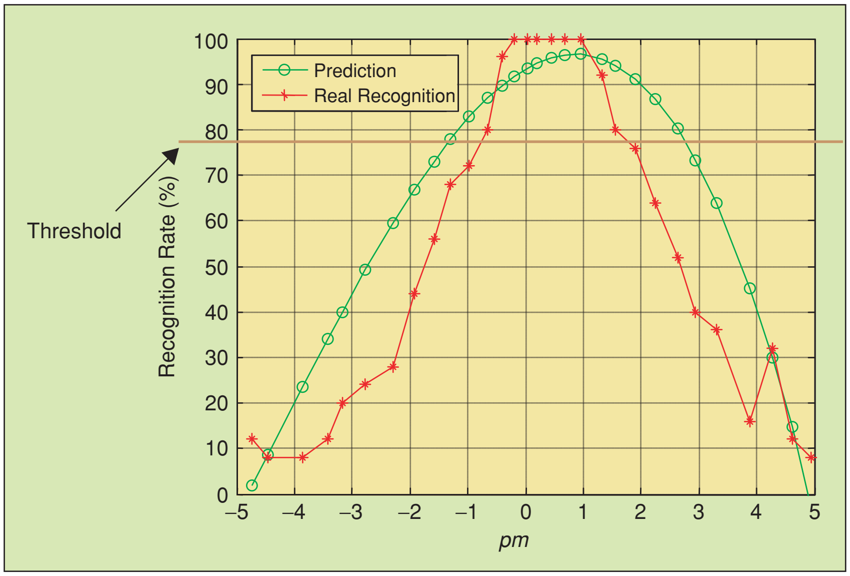

FIGURE 7 Recognition prediction rate and the real recognition versus head pose variations.

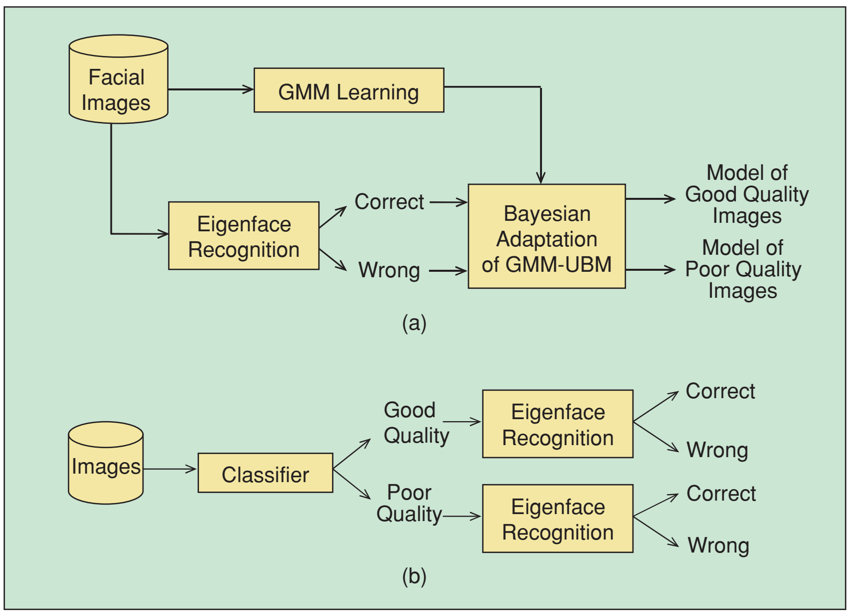

FIGURE 8 System diagram for assessing the quality of facial images with expressions: a) Training the GMM-UBM models, b) Testing the models for classification.

Next, we adapt the Gaussian Mixture Model (GMM) based on Universal Background Model (UBM) [16] to model these two classes of facial images. During the image assessment phase, for a given test image, we use the GMM-UBM models to classify the facial image with respect to face recognition into one of the two classes, i.e., good quality or poor quality. The GMM based on UBM has been successfully applied to speaker verification [16]. In fact the UBM is a background model that is trained using all the samples from all the classes (in this work we have two classes, the "Good quality" and the "Poor quality"). Then, after training the UBM, the background model is adapted for each individual class by using the sample data from that class. The GMM of all training samples is referred to as the Universal Background model, while the GMM corresponding to a sub-class is called a sub-model. A GMM consists of a weighted sum of L Gaussians. The model may be represented by:

$$\lambda = \{w_i, \mu_i, \Sigma_i\}, \ i = 1, \ldots, L \quad (6)$$

where μ_i and Σ_i represent the mean and covariance of each Gaussian and w_i represents its weight. Let $\bar{x}$ denote a feature vector of length D, then the probability of the feature vector $\bar{x}$ given the model λ is defined as:

$$p(\bar{x}|\lambda) = \sum_{i=1}^{L} w_i p_i(\bar{x}) \quad (7)$$

where each $p_i(\bar{x})$ is a single Gaussian distribution:

$$p_i(\bar{x}) = \frac{1}{(2\pi)^{D/2}|\Sigma_i|^{1/2}} \times \exp[-\frac{1}{2}(\bar{x}-\mu_i)^t \Sigma_i^{-1} \times (\bar{x}-\mu_i)] \quad (8)$$

The training of the GMM is usually implemented using Expectation-Maximization (EM) from an initial model [16]. We used this approach for training the Universal Background Model. During testing, as shown in Figure 8(b), for a given test image, we classify it as either belonging to the class of images with good quality or to the class of images with poor quality. This is achieved using the GMMs of each of the two classes and the *Maximum Likelihood* decision rule.

III. Experiments and Results

In this paper, we used several face databases such as the FERET database [15], the face database from West Virginia University [11], and the Cohn-Kanade face database [9] to evaluate our algorithms for face quality assessment. In the following subsections, we describe the content of each database and then we present our results and experiments. In this work, each database is split into two parts, one half for training and the other half for testing.

A. The Facial Image Databases Used in This Work

We used the gray scale images in the FERET database to evaluate our algorithm for predicting the face recognition rate of the Eigenface technique on images with blurring effect. 450 frontal gray scale images for 150 different subjects were selected from the FERET database. Figure 9 shows a sample set of images in this database.

The WVU database has two albums. The first album contains frontal color facial images of 50 subjects with variations in lighting conditions. For each subject, the light source rotates around the face from left (−90 degrees) to right (+90 degrees) and a video clip with 35 frames is captured. Figure 10 shows a sample set of images for one subject in the first album. The second album contains color images of 50 subjects with variations in head pose. For each subject, the camera rotates around the face from left (−45 degrees) to right (+45 degrees) and captures 30 images. Figure 11 shows sample of images for one subject in the second album.

To evaluate our algorithm for assessing the quality of facial images with facial expressions, we use the Cohn-Kanade face database which includes 97 subjects with different facial expressions captured in video sequences (gray scale images). Each sequence starts with a neutral face expression and the expression's intensity increases toward the end of the sequence. Figure 12 shows a sequence of images for one subject with joy facial expressions from Cohn-Kanade database.

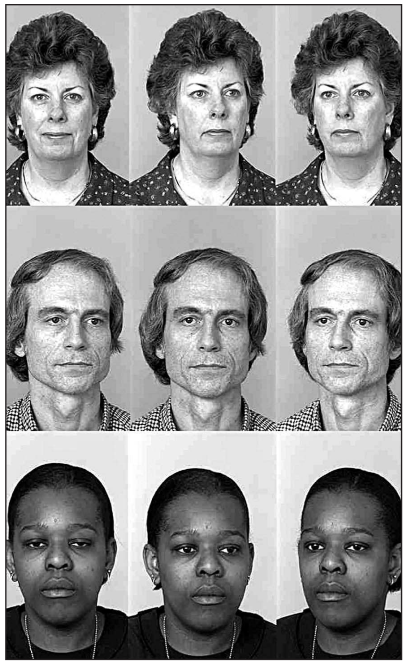

FIGURE 9 Sample of gray scale images for 3 subjects in FERET database.

B. Evaluation of Our Algorithms for Facial Image Assessment

To evaluate our algorithm for assessing the quality of facial images with respect to blurring effect, a subset of the FERET database was utilized and split into two separate sets of equal sizes for the training and the testing phases. During the training phase, we used a Gaussian filter to artificially blur the neutral facial images in the training set. Different values for σ, the standard deviation of the Gaussian filter, were used to obtain for each image a set of images with different levels of blurriness. For each of the resulting images, we calculated the Kurtosis and we applied the Eigenface technique and used the results to obtain Figure 3. We applied regression to the data in Figure 3 to obtain the coefficients of the prediction function. During the testing phase, we artificially blurred the images in the testing set and we calculated the Kurtosis. After that, we estimated the recognition prediction rate for the blurred images by utilizing the Kurtosis measure in the prediction function and also we applied the Eigenface technique to obtain the actual recognition results. Therefore, for each blurred image in the testing set, we determined the recognition prediction rate of the image and the exact recognition result of the Eigenface technique. Now, by choosing a threshold for the recognition prediction rate, we accept the images with a recognition prediction rate higher than the threshold as "Good Quality" images for recognition and reject the images with a recognition prediction rate lower than the threshold as "Poor Quality" images for recognition. By comparing these results with the exact recognition results of the Eigenface, we can evaluate the capability of our prediction function for assessing the quality of facial images effected by blurriness. Figure 13 shows the error between the predicted recognition and the actual recognition for different threshold levels of the prediction rate. As the Figure shows, when choosing a lower threshold level, we accept images with "Poor Quality" (i.e., images with

FIGURE 10 Uniformly sampled sequence of images with different lighting conditions (the first album of WVU).

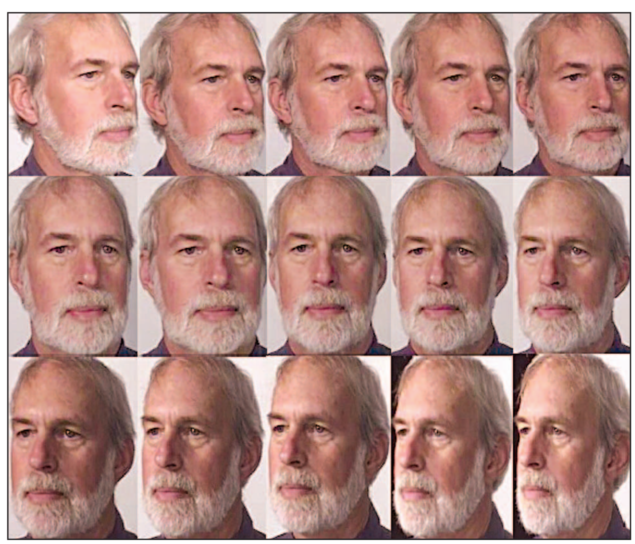

FIGURE 11 Uniformly sampled sequence of images for one subject with head pose variations (the second album of WVU).

higher blurring effect) and consequently the error rate becomes high.

We used the first album of the WVU database to test our approach for assessing the effect of lighting conditions. During the training phase, for the images of each subject in the training set we calculated the *wmi* feature. Moreover, we applied the Eigenface technique to the images in the training set to obtain the prediction function. During the testing phase, we calculated the *wmi* feature for each image in the testing set and used the proposed prediction function to predict the recognition rate of the Eigenface technique from the calculated *wmi*. Also, we applied the Eigenface technique to all the images in the testing set. Now, by choosing a threshold for the recognition prediction rate, we accept the images with the recognition prediction rate higher than the threshold level as "Good Quality" images for recognition and reject the images with a recognition prediction rate lower than the threshold as "Poor Quality" images for recognition. Figure 14 shows the error between the predicted recognition and the actual recognition for different threshold levels of the prediction rate. As Figure 14 shows, when choosing a lower threshold level, (i.e., lower prediction recognition rate) we accept images with "Poor Quality" (i.e., images with poor illumination) for recognition and consequently the actual error rate becomes high.

The second album of WVU face database was used for evaluating our algorithm for assessing the quality of facial images affected by head pose. We followed the same approach as for the blurring and lighting effects. During the training phase, we trained the coefficients of a prediction function to predict the recognition rate of the Eigenface technique versus the *pm* measure. During the testing phase, we calculated the

FIGURE 12 Images for joy facial expressions in Cohn-Kanade database.

TABLE 1 Classifier performance for different facial expressions.

		CORRECT CLASSIFICATION(%)	INCORRECT CLASSIFICATION(%)
GOOD QUALITY	JOY	73.66	26.34
	ANGER	67.68	32.32
	FEAR	81.25	18.75
	DISGUST	67.05	32.95
	SURPRISE	33.58	66.41
	SADNESS	61.46	38.54
POOR QUALITY	JOY	25.00	75.00
	ANGER	33.33	66.67
	FEAR	0.00	100.00
	DISGUST	37.50	62.50
	SURPRISE	6.45	93.55
	SADNESS	0.00	0.00

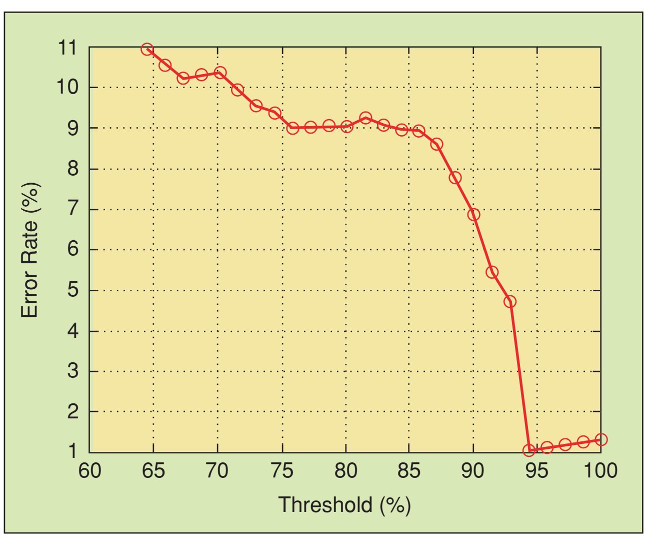

FIGURE 13 The error rate in the recognition prediction with respect to blurring.

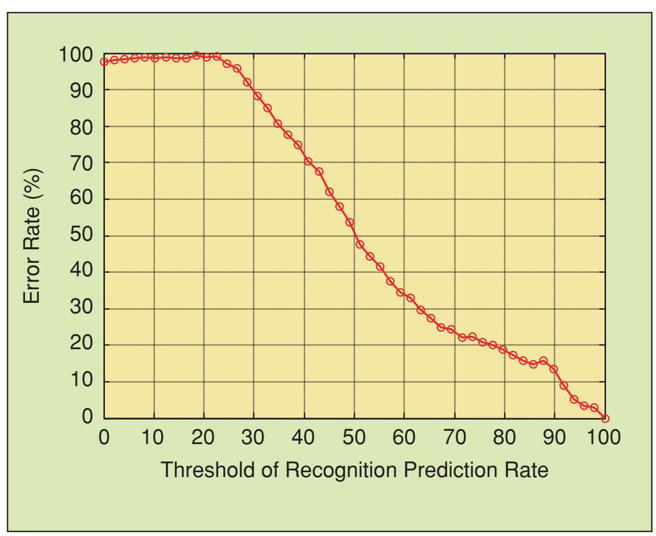

FIGURE 14 The error rate in the recognition prediction with respect to lighting conditions.

pm measure for each image in the testing set and used it to predict the recognition rate of the Eigenface technique using the proposed prediction function. Also, we applied the Eigenface technique to the images in the testing set to obtain the actual recognition results. Figure 15 shows the error between the predicted recognition and the actual recognition for different threshold levels of the prediction rate. Like the argument we had for the blurring and lighting conditions, by choosing a lower threshold level, we accept images with the "Poor Quality" for recognition and consequently the error rate becomes high.

To evaluate our algorithm for assessing the quality of facial images with respect to facial expressions, we split the Cohn-Kanade database into two separate sets of equal sizes for training and testing. For training the classifier, we need two sets of facial images. The first set includes images that are correctly recognized by the Eigenface technique. The second set includes images that the face recognition system fails to recognize. The two sets are obtained by applying the face recognition algorithm to all the images in the training set. We train the GMM-UBM model using the algorithm reviewed in Section II-D. For each subject and expression, we selected the frames of the neutral faces and the frames with high intensity expression for both training and testing the GMMs. Table 1 shows the performance of the classifier for assessing the quality of facial images with different expressions. Table 2 shows the total performance of the system. The net performance of the system (the weighted sum of True Positives and True Negatives) is about 75%. Also, our experiment shows that the surprise expression is the expression that has the highest degrading effect on the performance of the face recognition system. This is due to the fact that for the surprise expression the muscles in the upper and the lower parts of the face are deformed. In other words, the change in face appearance with the surprise expression is more than the change for the other expressions.

TABLE 2 Classifier performance.

	CLASSIFIER PERFORMANCE (GMM)%
TRUE POSITIVES	75.67
FALSE POSITIVES	29.03
TRUE NEGATIVES	70.97
FALSE NEGATIVES	24.33

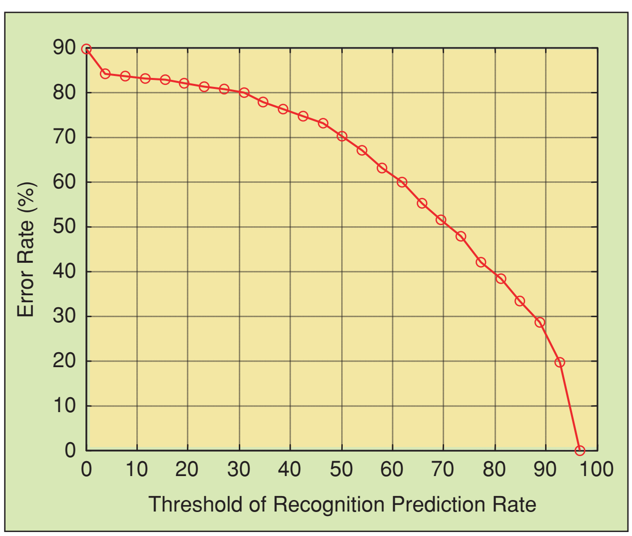

FIGURE 15 The error rate in the recognition prediction with respect to head pose.

IV. Conclusions and Future Works

In this paper, we presented algorithms to assess the quality of facial images affected by factors such as blurriness, lighting conditions, head pose variations, and facial expressions. We developed face recognition prediction functions for images affected by blurriness, lighting conditions, and head pose variations based upon the Eigenface technique. We also developed a classifier for images affected by facial expressions to assess their quality for recognition by the Eigenface technique. Our experiments using different facial image databases showed that our algorithms are capable of assessing the quality of facial images. These algorithms could be used in a module for facial image quality assessment in a face recognition system. In the future, we will integrate the different measures of image quality to produce a single measure that indicates the overall quality of a face image.

V. Acknowledgment

The authors would like to thank Dr. J. Cohn of University of Pittsburgh for providing the face expression database that was used in this work. Also, we would like to thank Dr. G. Fahmy of West Virginia University for providing the WVU face database. This work was supported in part through award from the NSF Center for Identification Technology Research (CITeR).

References

[1] "Biometric quality workshop," National Institute of Standards and Technology, March 2006.

[2] "Face recognition vendor test 2006," Available online at http://www.frvt.org, 2006.

[3] B.U.A. Hicklin and C. Watson, "The myth of goats: How many people have fingerprints that are hard to match?," NIST Interagency Report 7271, 2005.

[4] B. Fasel and J. Luettin, "Automatic facial expression analysis: A survey," *Pattern Recognition*, vol. 36, pp. 259–275, 2003.

[5] A. Hicklin and R. Khanna, "The role of data quality in biometric systems," Mitretek System, 2006.

[6] R. Hsu, M. Abdel-Mottaleb, and A. Jain, "Face detection in color images," *IEEE Trans. on Pattern Analysis and Machine Intelligence* , vol. 24, no. 5, pp. 696–706, May 2002.

[7] S. Joun, H. Kim, Y. Chung, and D. Ahn, "An experimental study on measuring image quality of infant fingerprints," in *LNCS, 2774*, pp. 1261–1269, 2003.

[8] N. Kalka, V. Dorairaj, Y. Shah, N.A. Schmid, and B. Cukic, "Image quality assessment for iris biometric," in In *Proc. of the Research Session, BCC*, 2005.

[9] T. Kanade, J. Cohn, and Y. Tian, "Comprehensive database for face expression analysis," in *Proceedings of the 4th IEEE International Conference of Automatic Face and Gesture Recognition (FG00)*, pp. 46–53, March 2000.

[10] S. Kotz and N. Johnson, "*Encyclopedia of statistical sciences*," in Wiely, pp. 415–426, 1982.

[11] S. Mandala, "The effect of lighting direction on face recognition performance," Msc Thesis, West Virginia University, Spring 2005.

[12] J. Moon and H. Kim, "Study on metrics for fingerprint image quality," in *Biometric Symposium*, 2004.

[13] T. Moore, "Cities opening more video surveillance eyes," *USA Today*, 7/18/2005.

[14] P.J. Phillips, P.J. Grother, R.J. Michaels, D.M. Blackburn, E. Tabassi, and J.M. Bone, "Face recognition vendor test 2002: Evaluation report," Available online at http://www.frvt.org, 2003.

[15] P.J. Phillips, H. Wechsler, J. Huang, and P. Rauss, "The feret database and evaluation procedure for face recognition algorithms," *Image and Vision Computing*, vol. 16, no. 5, pp. 295–306, 1998.

[16] D.A. Reynolds, T.F. Quatieri, and R.B. Dunn, "Speaker verification using adapted gaussian mixture models," *Digital Signal Processing*, vol. 10, pp. 19–41, 2000.

[17] E. Tabassi, C.L. Wilson, and C.I. Watson, "Fingerprint image qualit," NIST Interagency Report 7151, August 2004.

[18] M. Turk and A. Pentland, "Eigenfaces for recognition," *Journal of Cognitive Neuroscience*, vol. 3, no. 1, 1991.

[19] N.F. Zhang, M.T. Postek, R.D. Larrabee, A.E. Vladar, W.J. Kerry, and S.N. Josnes, "Image shapрness measurement in the scanning electron microscope part iii," *Scanning*, vol. 21, no. 4, pp. 246–252, July–August 1999.